A Novel Defect Diagnosis Method for Kyropoulos Process Based Sapphire Growth

Zhang, Wei; Qiao, Tiezhu; Pang, Yusong; Yang, Yi; Chen, Hong ; Hao, Guirong

DOI
10.1109/JSEN.2020.2969963

Publication date
2020

Document Version
Accepted author manuscript

Published in
IEEE Sensors Journal

A Novel Defect Diagnosis Method for Kyropoulos Process Based Sapphire Growth

Zhang, Wei; Qiao, Tiezhu; Pang, Yusong; Yang, Yi; Chen, Hong ; Hao, Guirong

DOI
10.1109/JSEN.2020.2969963

Publication date
2020

Document Version
Accepted author manuscript

Published in
IEEE Sensors Journal

This article has been accepted for publication in a future issue of this journal, but has not been fully edited. Content may change prior to final publication. Citation information: DOI 10.1109/JSEN.2020.2969963, IEEE Sensors Journal

A Novel Defect Diagnosis Method for Kyropoulos Process Based Sapphire Growth

Wei Zhang, Tiezhu Qiao, Yusong Pang, Yi Yang, Hong Chen, and Guirong Hao

***Abstract*—When sapphire crystal is prepared with Kyropoulos method, the necking-down growth process is a key stage. Sapphire growth defect is a big problem in this stage. However, diagnosing growth defects is subject to the interference of workers subjectivity and accuracy always goes down. To address the problem, a novel defect diagnosis method is proposed for necking-down growth process in this paper. Industrial CCD sensors replace eyes of skilled workers to observe in this method. A new Defect-Diagnosing Siamese network (DDSN) is used in this method. We use Siamese architecture to learn similarity through pairs of images. We use the deep separable convolution (DSC) into the DDSN to optimize running speed and model size. In experiment, dataset is acquired by industrial CCD sensors in the necking-down growth process. The accuracy of defect diagnosis can reach up to 94.5%. The method significantly improves the traditional way.**

***Index Terms*—CCD sensor, Defect-Diagnosing Siamese network, Necking-down process, Sapphire Growth Defects.**

I. INTRODUCTION

SAPPHIRE single crystal is an important industrial raw material, which has excellent physical properties, such as physical strength, chemical stability and thermal stability [1]. It is widely used in various fields, especially in some harsh environments. Sapphire has been used in many fields. C-plane sapphire is the ideal material for making light-emitting diodes (LEDs) [2] and sapphire can be used for bearing surfaces[3]. Kyropoulos (Ky) method is one of common methods for preparing sapphire [4], which is widely used because of its relatively low production cost. The process of preparing sapphire with the Ky method is as follows: 1) The material in the sapphire crucible is heated to complete melting, and the temperature is controlled at 2050°C (workers estimate temperature by voltage value in the equipment); 2) The control device lowers the seed rod so that the seed rod is inserted into the seed point of the melt; 3) The power of the device and the rotation speed of the seed rod are adjusted. The temperature is controlled so that the free surface temperature of the melt is at the melting point, and the crystal grows slowly; 4) In the process of the crystal necking-down growth, the pulling seed rod slowly rises while the seed crystal rotates to adjust the crystal to growing uniformly in all directions. Using of one or a few necking steps to avoid seed defects [5]. 5) The crystal forms a crystal neck and begins equal diameter growth. Meanwhile, temperature gradually decreases in the furnace. The melt gradually solidifies from top to bottom to form a single crystal ingot. The rate of good sapphire crystal can arrive at 90% in the industry studied.

In the preparation of sapphire, ensuring high quality sapphire production is an important technical task. The rate of good crystal is a core element of crystal quality. All stages are related to the rate of good crystal. Kim [6] proposed the use of image processing technology to develop an automatic seeding system in the process of growing the sapphire crystal by the Ky method. Yu [7] proposed the OCS method to detect the seeding point in the stage (2). Regarding the important stage (4) only human inspection is performed. The stage (4) is a key stage [8]. However, the stage (4) the accuracy of human diagnosis is subject to the interference of subjective factors and even low sometimes. Sapphire growth defects diagnosis is a challenge in this work.

Image processing has been used many times to study crystals. Kim studied the stage 2) to detect the seeding point [6]. Donecker studied the defect of crystal in micro level[9]. Chen researched on surface defect of crystal [10]. However, no one had studied the sapphire growth defects before using image processing in the stage 4). Traditionally, workers observed sapphire growth defects by the observation ports of crystal furnace in this stage. The growth defect is the surface of crystal which is connected by the seed rod. The structure of different crystal furnace is slightly different, and the intensity of the light is different in the furnace, which can stimulate the human eyes. The metal oxide vapor causes visual interference in the crystal furnace. The time of manual observation cannot be long, and

This work is supported by the National Natural Science Foundation of China-Shanxi coal-based low-carbon joint fund (Grant No. U1810121) and Key Research and Development Plan for Industrial Science and Technology Jinzhong City, Shanxi Province, China (Grant No. 201803D03111003) and High-end Foreign Expert Introduction Program (Grant No. G20190204013)

W. Zhang, T. Qiao and Y. Yang are with the Key Laboratory of Advanced Transducers and Intelligent Control System, Ministry of Education, Taiyuan University of Technology; the College of Physics and Optoelectronics, Taiyuan University of Technology, Shanxi 030000, China (e-mail: zw19930606@sina.com; qiaotiezhu@tyut.edu.cn; yangyi01@tyut.edu.cn).

Yusong Pang is with the section of Transport Engineering and Logistics, Delft University of Technology, the Netherlands (e-mail: y.pang@tudelft.nl)

H. Chen and G. Hao are with Shanxi Zhongjujingke Semiconductor Co., Ltd, Shanxi 030600, China (e-mail: 353881118@qq.com; 981946425@qq.com)

This article has been accepted for publication in a future issue of this journal, but has not been fully edited. Content may change prior to final publication. Citation information: DOI 10.1109/JSEN.2020.2969963, IEEE Sensors Journal

growth defects cannot be observed in time. Hence, CCD sensors are used to replace eyes of workers in this work. The CCD sensors can acquire images connected with the observation ports. In addition, manual diagnosis is based on human experience. Even if the workers can find the defects, it is difficult for skilled workers to judge directly. It will spend a lot of time. Therefore, we use deep learning to simulate human experience. Deep learning is widely used in image classification. However, it has never been used to diagnose sapphire growth defects based on large data before. Aiming at diagnosing growth defects accurately, this paper proposes a novel defect diagnosis method. This method uses CCD sensor to observe and acquire images. In addition, this method uses a Defect-Diagnosing Siamese network (DDSN) to diagnose sapphire growth defects. The DDSN is suitable for sapphire necking-down growth to perform on-line diagnosis of growth defect, thereby ensuring the superiority of crystal quality. The on-line diagnosis is that the computer runs continuously and diagnose defects in real time. We combine the Siamese architecture with depth separable convolution (DSC). First, this method utilizes a Siamese architecture for similarity learning. Second, because industrial environment requires good real-time performance for diagnosis, our method uses DSC to extract features for real-time diagnosis. This is the first diagnosis method in diagnosing sapphire growth defects. In this paper, the goal is to accurately diagnose sapphire growth defects, and thus ensure a good rate of good sapphire crystals.

The rest of the paper is organized as follows: section 2 describes the related work of sapphire growth defect and our architecture. Section 3 details the proposed method. Section 4 shows the experiment and result. Section 5 concludes this work.

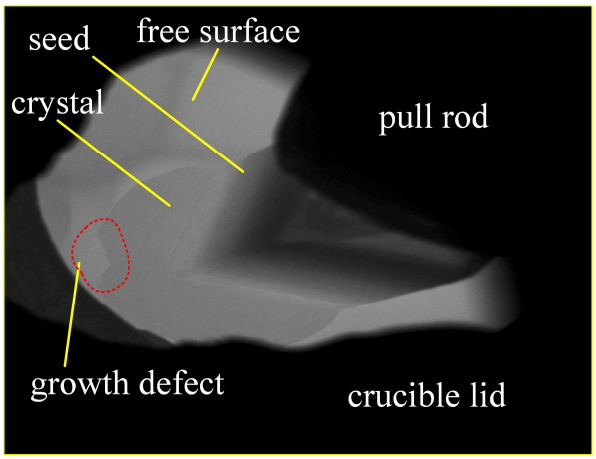

(a)

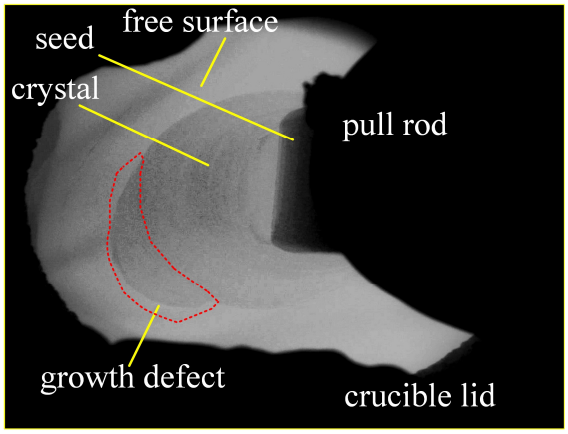

(b)

(c)

Fig. 1. Sapphire growth defect and crystal defect (a) The image of growth defect(concave). (b) The image of growth defect(convex). (b) Crystal defect.

II. Related Work

The DDSN is a new network in diagnosing growth defect, and it has a direct link to the quality of the final sapphire crystal. If sapphire growth defects occur during the necking-down growth process, the rate of good crystal will drop or even crystals can't form in the furnace. The traditional method has drawbacks in terms of diagnosis accuracy. In this work, we use deep learning to diagnose and analyze sapphire growth defect, which shows the advantages of our method in the field. In this section, we mainly talk about relevance from the following two aspects.

A. Sapphire growth defect

In the work of Kim. and Yu., using images to find sapphire seeding points has made a lot of efforts [13,14], but there are still many challenges and unresolved problems in the field of sapphire preparation. Diagnosis of sapphire growth defect is one of those problems. Sapphire growth defect can generate final crystal defects.

Crystal defects are often difficult to avoid, and they include microscopic and macroscopic defects. Workers try to minimize the occurrence of defects in the macro [11]. As shown in Fig1.

(a) and Fig1. (b), the growth defects are surrounded by the red dotted line. The growth defects are part of crystal. The non-ellipse growth images are defined as growth defects. The top of crucible is a part of crucible lid, which covers a part of the perspective. The crystal is located between the seed crystal and the free surface, which has growth defects. In physics, a free surface is the surface of a fluid that is subject to constant perpendicular normal stress and zero parallel shear stress. When the growth defects are observed by the naked eye in the necking-down growth stage, and if crystal defects are not treated, the final sapphire crystal will have obvious defects in Fig.1 (c). These obvious crystal defects include cracks and abnormal growth [12].

The development of modern science requires highly intact crystals. In order to obtain good physical properties, it is necessary to grow crystals with good integrity and strictly control the content of impurity and defect. The form of sapphire growth defects is due to the uneven distribution of the temperature field in the crystal reactor after sapphire seeding [13] and the uneven concentration distribution of each component. The seed crystal is deformed during the growth process, and has a shape such as a concave or a convex, as shown in Fig.1 (a) and (b). Here we define these deformations as sapphire growth defects. The main reason for these growth defects is that an ideal transmission device is needed to enable the crystal or crucible to rotate stably and vertically, and the ideal stable control system in the process of growing sapphire by Ky method. However, the transmission device of the growth device cannot be completely idealized, and the accuracy of the temperature control system is not particularly good. Some mechanical vibrations of the transmission device and sudden changes in the rate of rise and fall of the seed crystal rod, and changes in heating power and heat dissipation power lead to the fluctuation of crystal growth rate. These will cause the occurrence of growth defects. Growth defects in the necking-down growth process will lead to the final crystal defects. An important task of workers is to grow a single sapphire crystal material with less defects or even no defect with the optimal composition in the optimal growth conditions.

B. The description of our architecture

Deep learning has applications in other field, such as fault diagnosis [14] and activity recognition in a smart home [15]. Deep learning convolutional networks can extract dimensional features. In this paper, we use the Siamese architecture to build a new architecture. It learns similarity through pair of images and can achieve better image matching. Siamese architecture has achieved some good results in the fields of face recognition [16], handwriting recognition [17], and video tracking [18]. Zhang [16] proposed a deep disentangling Siamese network for frontal face synthesis. Those methods use the Siamese network, but they are not mentioned in terms of speed, and are not friendly to the industrial environment. Therefore, our approach adds deep separable convolutions in the network to optimize the running speed. Google demonstrated DSC in the MobileNet for mobile and embedded devices [19]. The combination of MobileNet and Faster R-CNN was used to ensure real-time performance while achieving high accuracy [20]. Li [21] proposed a surface defect detection algorithm based on MobileNet-SSD to detect the defects accurately and rapidly.

We propose a DDSN for Sapphire Growth Defect. In order to meet the actual industrial requirements, the DDSN combined the Siamese architecture with DSC for better results. The use of DDSN for image matching has considerable advantages. It only needs to use a small quantity of data to train the model, and attains high classification effect.

III. DEFECT-DIAGNOSING SIAMESE NETWORK

A. Building A Deep Learning Network

Deep learning can simulate human experience. According to the sapphire necking-down growth process, we divide the acquired images into two states: defective and healthy. We build a deep learning network, which not only applies to the small sample size of the sapphire growth process, but also improves the diagnosis speed. The network is based on a combination of DSC and a Siamese architecture on the TensorFlow framework [22]. The purpose of DSC is to solve the standard convolution kernel into depthwise convolution (DWC) and pointwise convolution (PWC). The PWC is used to connect different channels of the DSC, which can increase the number of channels and can significantly reduce the amount of calculation compared the standard convolution kernel. The DSC can optimize running speed and model size. The number of input channels is M, and the number of output channels is N. The corresponding calculation amount is: $P_K \times P_K \times M \times N \times P_F \times P_F$, where P_K and P_F are the spatial width and height of a square output feature map.

The calculation amount of DWC and PWC is $P_K \times P_K \times M \times P_F \times P_F + M \times N \times P_F \times P_F$ The calculation amount has been reduced [19] :

$$\frac{P_K \times P_K \times M \times P_F \times P_F + M \times N \times P_F \times P_F}{P_K \times P_K \times M \times N \times P_F \times P_F} = \frac{1}{N} + \frac{1}{P_K^2} \quad (1)$$

The DSC replaces the traditional convolution, which greatly reduces the amounts of parameters and the amount of calculation. This network structure can improve the operation speed, and it can process data in real time on the CPU. The DSC makes a good foundation for the practical application in industry.

The Siamese architecture can learn the similarity of pictures. The main idea of the Siamese architecture is to map to the target space through a function, and use the Euclidean distance to match the similarity in the target. The left and right sides are identical network structures and share the weight W. The data inputted is not an image but a pair of images: (X_1, X_2, Y), where $Y = 0$ means that X_1 and X_2 do not belong to the same sapphire state, $Y = 1$ indicates the same state. The same pair is $(X_1, X_2, 1)$, and the different pair is $(X_1, X_2, 0)$.

The loss function of the DDSN contains the classification loss of the sample. The loss function formula is as follows [16] :

$$\mathrm{L_c} = Y \| Q_1 - Q_2 \|_2^2 + (1-Y)\max(m\arg in - \| Q_1 - Q_2 \|_2^2, 0)^2 \quad (2)$$

Where Q_1 and Q_2 are the Euclidean distance of output in the Siamese network. The margin parameter is the margin value,

This article has been accepted for publication in a future issue of this journal, but has not been fully edited. Content may change prior to final publication. Citation information: DOI 10.1109/JSEN.2020.2969963, IEEE Sensors Journal

which should be greater than zero. Y is a label of our image, which should be one or zero.

The architecture has one 3×3 convolutional layer, thirteen 1×1 convolutional layers, thirteen deep separable convolutional layers and a fully connected layer. These layers can extract feature of pictures. The architecture is to predict the category of the input image. In the last layer of the classification part, all neurons are connected to the output. The last layer has the softmax activation function [23]. At the end of the convolutional layers and depth separable convolutional layers, the ReLu functions are used. The ReLu function can make part of the neurons output as zero, which can result in good sparsity of the network and prevent over-fitting. As shown in Fig.2 (a), the Conv, DWC, Pool, FC1, and Softmax represent the convolutional layer, depth separable convolutional layer, pooling layer, fully connected layer, and softmax layer respectively. The convolutional layers and depth separable convolutional layers are the core of convolutional neural network, and most operations are carried out on the convolutional layers. The mathematical operation is convolution operation to extract various features in the convolutional layers. The pooling layer can reduce the dimension of features. The fully connected layer can combine the extracted local features. Softmax layer can classify the extracted features.

As shown in Fig. 2 (a), the proposed network structure is composed of DSC and Siamese architecture. The loss function of this Siamese architecture can learn to implement a good classification function, calculate the Euclidean distance between the two images and encourage the matching pairs to be very close in the feature space. The non-matching distance is very far in the feature space. To make similarity learning easier, the paper uses the DSC to map the original image to the lower dimension. The feature is reduced from the high-dimensional feature to the low-dimensional feature to learn a similarity measure. As shown in Fig. 2 (b), the trained network input image is tested to finally obtain a prediction of the image category.

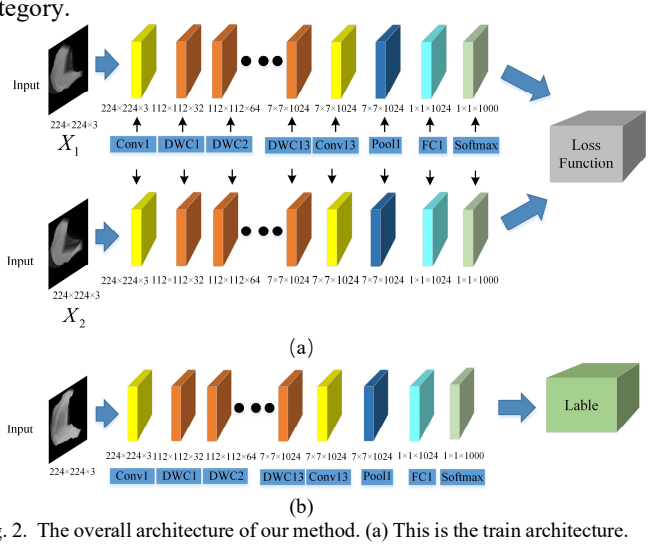

Fig. 2. The overall architecture of our method. (a) This is the train architecture. The architecture has one 3×3 convolutional layer, thirteen 1×1 convolutional layer, thirteen deep separable convolutional layers a pooling layer and a fully connected layer. The input size is below the layers. (b) This is the test architecture. The architecture is the same as one branch of the train architecture.

B. *Network Training*

The dataset is acquired by the industrial CCD sensors and the dataset of growth defects is established. The dataset contains both healthy and defective samples. Some of these data are in the Fig. 3. Fig. 3 shows the richness of the data. The healthy images were acquired at different times and furnaces in Fig. 3 (a). The defective images were acquired at different times and furnaces in Fig. 3 (b). In addition, the dataset includes images of same growth defect, which were acquired in different times in Fig. 3 (c). These improve the dataset and increase the reliability of dataset.

Due to some metal oxide vapor in the crystal furnace, the histogram equalization method is applied for image processing to enhance the image before using these image data. Histogram equalization is a nonlinear stretching of the image, which redistributes the pixel values to the pixels in the image and makes the pixel values in the grayscale range approximately equal in Fig. 4. It can improve the contrast of the image to facilitate deep learning of the network learning feature.

There were twelve reaction furnaces selected randomly from all industrial furnaces. We divided images collected into two categories, which were positive and negative. The positive samples are healthy and the negative samples are defective. In this experiment, there were 3000 negative images and positive image groups, which were divided into training set and test set. We used 2600 sets of images as training set, and used extra 400 sets of images as test set randomly. We set the margin parameter to 5. The RMSprop [24] optimization algorithm is used during training, with momentum parameter of 0.9 and learning rate of 0.003. It took about 3 hours for the process.

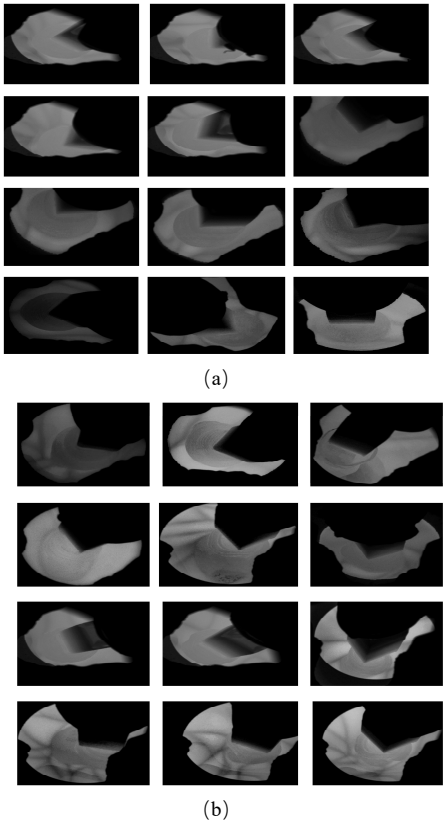

This article has been accepted for publication in a future issue of this journal, but has not been fully edited. Content may change prior to final publication. Citation information: DOI 10.1109/JSEN.2020.2969963, IEEE Sensors Journal

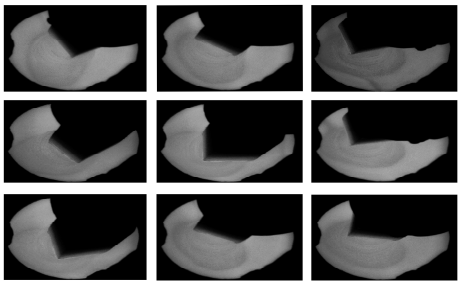

(c)

Fig.3. Growth sapphire in different states. (a) The no-defect images of sapphire growth. (b) The defective images of sapphire growth. (c) The same growth defect in different times in the furnace as the seed rod rotates.

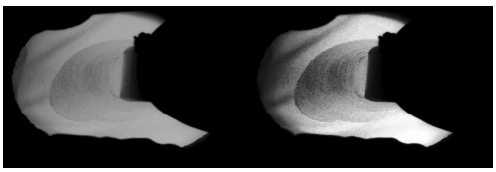

Fig. 4. Comparison chart before and after histogram equalization.

IV. Experiment And Result

The running environment of PC is performed on TensorFlow under window10. The hardware environment used is Intel I5-8400, 16G-CPU, and the graphics card is Nvidia GeForce GTX1060. In this work, the input images were resized to 224×224 for ease of processing. The experimental platform for collecting image data is shown in Fig. 5 (a). In order to ensure the stability of the CCD sensor, the CCD sensor is fixed with a magnetic seat.

In Fig. 5 (b), there are two CCD sensors, which are industrial CCD FLIR GS3-U3-14S5C. The CCD sensor collects image data through the observation port of the crystal reaction furnace, and stores the data in a PC. After the image data is acquired by the CCD sensor, the driver device is controlled by the PLC to perform corresponding operations on the seed rod (elevating and rotating the seed rod). The driver device includes stepping motors and other machinery to control pull rod. The flow chart of experiment is in Fig. 5 (c).

Before the experiment, the CCD sensors need to be configured and calibrated. The value of exposure and the value of Brightness are set to the lowest due to the intensity of the light is too high in the furnace. Other parameter settings are adjusted according to specific conditions. The grayscale color mode is used to clearly show images compared with other colors.

Before training our network, we need to make image pairs based on the Siamese architecture. The positive image pair $(X_1, X_2, Y=0)$ and the negative image pair $(X_1, X_2, Y=1)$ are generated as follows: according to the acquired X_1 and X_2 images, the collected images are classified according to the presence or absence of defects. For the positive and negative groups, they are combined by computer to make a data set. After screening, the images are cross-combined and stored production data set in the positive group and the negative group in the production of our dataset.

Fig. 6 shows the performance of the classifier. We apply the trained model to the test architecture to test the performance on the test set. It is a binary classifier. Their classification is based on feature descriptors learned by neural networks. We use the red and blue dots to show the result of classification. Those dots represent the distribution of images of test set in 2-dimension. The horizontal and vertical coordinates represent numerical values without practical significance. The healthy images and defective images are classified by red dots and blue dots in Fig. 6, respectively. The black line is the linear classification boundary. The linear classification boundary, based on the classification result of classifier, is good classification boundary. The softmax classifier is based on the softmax function [23]. The output of classifier is the range of (0,1). The value of output something like a probability value. The ratio of the misclassification in the overall samples is the accuracy rate. It can show the performance of the classifier.

The accuracy shows the ratio of the healthy samples in all samples. The formula of accuracy is followed:

$$Accuracy = \frac{A}{B} \tag{3}$$

Where A indicates the number of samples with the correct classification and B is the number of all samples. In the experiment, A is 378 and B is 400. As a result, the accuracy rate of model can arrive at 94.5% in this work.

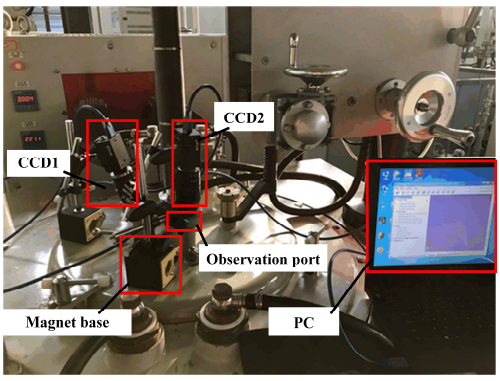

(a)

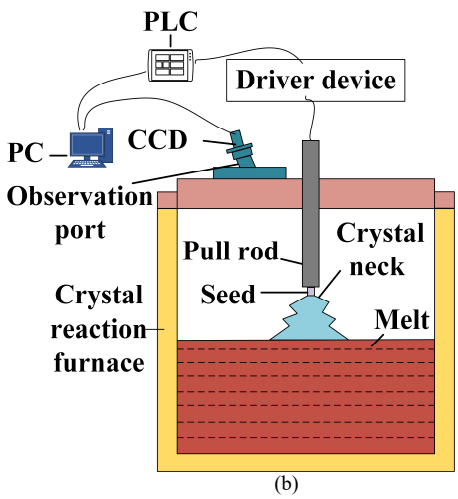

(b)

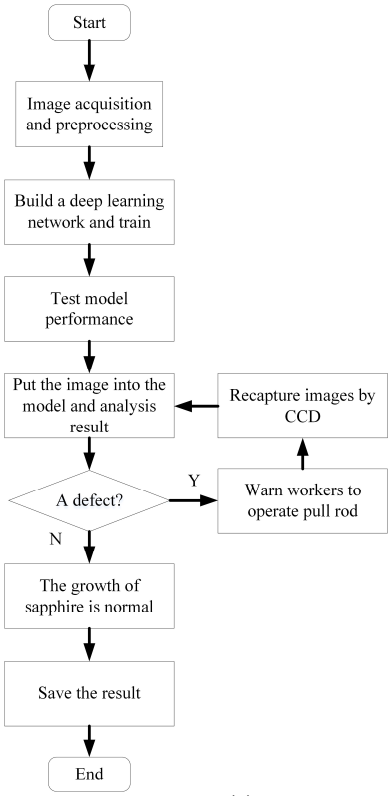

(c)

Fig. 5. Experimental setup and flow chart. (a) The experiment platform. (b) Overall schematic of the diagnosis device. (c) Experimental flow chart.

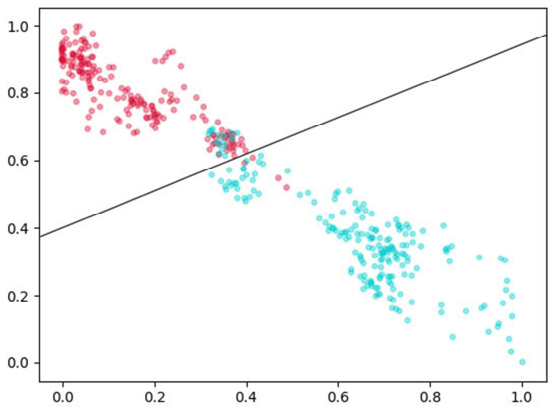

Fig.6. Performance of classifier.

V. Conclusion

In this paper, a novel defect diagnosis method is presented. Current observation and diagnose of defects rely on human being. These defects are difficult to observe and diagnose. Traditional way can be replaced by automated observation via CCD and the diagnosis can be done by deep learning. This method uses a DDSN for diagnosing sapphire growth defects in the necking-down process. The proposed method can be applied for accurate defect diagnoses. The method can diagnose sapphire growth defects and arrive high accuracy rate at 94.5% in necking-down growth process. Our future work will focus on diagnosing defects of all growth process.

References

[1] M. Sui, P. Pandey, M. Y. Li, Q. Zhang, S. Kunwar, and J. Lee, "Au-assisted fabrication of nano-holes on c-plane sapphire via thermal treatment guided by Au nanoparticles as catalysts," *Appl. Surf. Sci.*, vol. 393, pp. 23–29, 2017.

[2] F. Scholz *et al.*, "Semipolar GaN-based heterostructures on foreign substrates," *Phys. Status Solidi Basic Res.*, vol. 253, no. 1, pp. 13–22, 2016.

[3] O. A. Rozenberg, R. Turmanidze, S. V. Sokhan, and V. V. Voznyy, "Bearing Surfaces with Sapphire for Total Hip-Joint Replacement," *Key Eng. Mater.*, vol. 496, pp. 121–126, 2012.

[4] A. Nehari *et al.*, "Ti-doped sapphire (Al2O3) single crystals grown by the kyropoulos technique and optical characterizations," *Cryst. Growth Des.*, vol. 11, no. 2, pp. 445–448, 2011.

[5] C. Of and S. Ribbon, "GROWTH AND CHARACTERIZATION OF SAPPHIRE RIBBON CRYSTALS Kazumi WADA and Keigo HOSHIKAWA," vol. 50, pp. 151–159, 1980.

[6] C. Kim, S. Kim, and J. Ahn, "Development of Auto-Seeding System Using Image Processing Technology in the Sapphire Crystal Growth Process via the Kyropoulos Method," *Appl. Sci.*, vol. 7, no. 4, p. 371, 2017.

[7] B. Yu, T. Qiao, H. Zhang, and G. Yan, "The OCS method of seeding point detection using visible vision for large-diameter sapphire single crystal growth via the Kyropoulos method," *Meas. J. Int. Meas. Confed.*, vol. 137, pp. 39–48, 2019.

[8] J. Of and S. Ic, "m ical B onding Theory of the C rystal G row th," 2006.

[9] J Donecker,."Defect Recognition and Image Processing in Semiconductors 1997: Proceedings of the seventh conference on Defect Recognition and Image Processing, Berlin, September 1997. Routledge, ", 2017.

[10] "Defect Inspection of Quartz Crystal Based on Machine Vision," vol. 9045, pp. 1–8, 2013.

[11] W. Balluffi, "<R W Balluffi Introduction to elasticity theory for crystal defects 2012.pdf>," 2012.

[12] F. Jiang, X. Luan, N. Wang, X. Xu, X. Lu, and Q. Wen, "Research on the dynamic mechanical properties of C-plane sapphire under impact loading," *Ceram. Int.*, vol. 44, no. 8, pp. 9839–9847, 2018.

[13] S. E. Demina *et al.*, "Numerical analysis of sapphire crystal growth by the Kyropoulos technique," *Opt. Mater. (Amst).*, vol. 30, no. 1, pp. 62–65, 2007.

[14] M. Sadoughi and C. Hu, "Physics-Based Convolutional Neural Network for Fault Diagnosis of Rolling Element Bearings," *IEEE Sens. J.*, vol. 19, no. 11, pp. 4181–4192, 2019.

[15] T. H. Tan, M. Gochoo, S. C. Huang, Y. H. Liu, S. H. Liu, and Y. F. Huang, "Multi-resident activity recognition in a smart home using RGB activity image and DCNN," *IEEE Sens. J.*, vol. 18, no. 23, pp. 9718–9727, 2018.

[16] T. Zhang, H. Wang, and Q. Dong, "Deep disentangling siamese network for frontal face synthesis under neutral illumination," *IEEE Signal Process. Lett.*, vol. 25, no. 9, pp. 1344–1348, 2018.

[17] G. Koch and G. Koch, "Siamese Thesis," 2015.

[18] R. Tao, E. Gavves, and A. W. M. Smeulders, "Siamese instance search for tracking," *Proc. IEEE Comput. Soc. Conf. Comput. Vis. Pattern Recognit.*, vol. 2016-Decem, pp. 1420–1429, 2016.

[19] A. G. Howard *et al.*, "MobileNets: Efficient Convolutional Neural Networks for Mobile Vision Applications," 2017.

[20] J. Li and Z. Wang, "Real-Time Traffic Sign Recognition Based on Efficient CNNs in the Wild," *IEEE Trans. Intell. Transp. Syst.*, vol. 20, no. 3, pp. 975–984, 2019.

[21] Y. Li, H. Huang, Q. Xie, L. Yao, and Q. Chen, "Research on a Surface Defect Detection Algorithm Based on MobileNet-SSD," *Appl. Sci.*, vol. 8, no. 9, p. 1678, 2018.

[22] C. Core, *12 Large-Scale Machine Learning*. 2017.

[23] X. Cao, R. Togneri, X. Zhang, and Y. Yu, "Convolutional Neural Network with Second-Order Pooling for Underwater Target Classification," *IEEE Sens. J.*, vol. 19, no. 8, pp. 3058–3066, 2019.

[24] S. Roy, N. Das, M. Kundu, and M. Nasipuri, "Handwritten isolated Bangla compound character recognition: A new benchmark using a novel deep learning approach," *Pattern Recognit. Lett.*, vol. 90, pp. 15–21, 2017.

This article has been accepted for publication in a future issue of this journal, but has not been fully edited. Content may change prior to final publication. Citation information: DOI 10.1109/JSEN.2020.2969963, IEEE Sensors Journal

WEI ZHANG received the B.S. degree in automation from Lanzhou University of Technology, Lanzhou, China, in 2016. He is currently pursuing the M.S. degree in integrated circuit engineering with the Taiyuan University of Technology, Taiyuan, China. His research interests include image processing, deep learning and coal defect detection.

TIEZHU QIAO received the B.S. degree in industrial electrical automation from Shanxi Mining Institute in 1990, the M.S. degree in control science and engineering from Taiyuan University of Technology in 2004 and the Ph.D. degree in circuits and systems from Taiyuan University of Technology, Taiyuan, China, in 2015.

He is currently a Professor and the director of the Key Laboratory of Advanced Transducers and Intelligent Control System, Ministry of Education, Taiyuan University of Technology, Taiyuan, China. His research interests include machine vision, advanced transducers, and intelligent control system.

YUSONG PANG received his MSc degree in Electrical Engineering in 1996. From 2000 he started working at Seaview B.V. the Netherlands for industrial production life cycle management. After his PhD research of Intelligent Belt Conveyor Monitoring and Control in 2007, he was employed at the Advisory Group Industrial Installations of Royal Haskoning the Netherlands as an Expert Material Handling. From 2010 he started working as an assistant professor in the section of Transport Engineering and Logistics, Delft University of Technology, the Netherlands. His research mainly focuses on the intelligent control for large-scale material handling systems and logistics processes.

YI YANG received the Ph.D. degree in instrument science and technology from Tianjin University, Tianjin, China, in 2018. He is currently working at the Key Laboratory of Advanced Transducers and Intelligent Control System, Ministry of Education, Taiyuan University of Technology, Taiyuan, China. His research interests include computer vision, image processing, and pattern recognition.

HONG CHEN is president of Shanxi Zhongjujingke Semiconductor Co., Ltd. The business scope of company includes research and development, production and sales of sapphire crystals. The company have a complete industrial chain from production to application.

GUIRONG HAO is vice-general manager of Shanxi Zhongjujingke Semiconductor Co., Ltd. The business scope of company includes research and development, production and sales of sapphire crystals. The company have a complete industrial chain from production to application.